research papers

COHbC and COHbS crystallize in the R2 quaternary state at neutral pH in the presence of PEG 4000

Larysa N. Patskovska,[a] Yury V. Patskovsky,[b] Steven C. Almo[b]* and Rhoda Elison Hirsch[a,c]*

[a]Department of Medicine (Division of Hematology), Albert Einstein College of Medicine, Bronx, New York, USA, [b]Department of Biochemistry, Albert Einstein College of Medicine, Bronx, New York, USA, and [c]Department of Anatomy and Structural Biology, Albert Einstein College of Medicine, Bronx, New York, USA

Correspondence e-mail: almo@aecom.yu.edu, rhirsch@aecom.yu.edu

Human hemoglobin binds oxygen cooperatively and functions as a tetramer composed of two identical $\alpha\beta$ heterodimers. While human hemoglobin is the best characterized allosteric protein, the quaternary R (oxygenated or liganded) to T (deoxygenated) structural transition remains controversial. The R2 state has been postulated to represent either an intermediate or final quaternary state elicited by ligand binding. However, the biological relevance of the R2 state has been questioned as it has not been observed crystallographically under physiological conditions. The high-resolution R2 quaternary structures of human COHbC (βE6K) and COHbS (βE6V) are reported at neutral pH and low ionic strength using PEG 4000 as a precipitant. Crystals of COHbC, COHbS and their mixtures are isomorphous, indicating that they share the same tertiary and quaternary structures. In contrast, oxyHbA or COHbA did not yield crystals at neutral pH under similar conditions. Solubility studies and modeling suggest that at neutral pH and low ionic strength the $\beta6$ mutant hemoglobins crystallize (βK6 > βV6) as a result of more favorable lattice contacts.

1. Introduction

Human hemoglobin (Hb) binds oxygen cooperatively and functions as a tetramer of two identical $\alpha\beta$ heterodimers. Hemoglobin is perhaps the most extensively studied allosteric protein, yet significant questions concerning the oxygenated to deoxygenated structural transition remain unresolved. The classic two-state model allosteric transition predicted by Monod *et al.* (1965) invokes the liganded or R (relaxed) form and the deoxygenated or T (tense) form, and gained early support from the crystallographic work of Perutz (1970). Alternatively, Koshland *et al.* (1966) proposed an allosteric model based upon a sequential change during the R to T transition requiring distinct intermediate states. Over the years, thermodynamic and ligand-binding studies from many laboratories have provided evidence favoring one model or the other.

Structures of human oxy and carbonmonoxy (CO) HbA designated as R state were solved using crystals grown from concentrated phosphate buffers [*e.g.* PDB entries 1hho, 1ljw, 1fsx, 1rvw and 1k1k (Shaanan, 1983; Safo *et al.*, 2002; Safo & Abraham, 2001; Puius *et al.*, 1998; Dewan *et al.*, 2002)]. COHbA is frequently used as a model of the R state since it is more stable than oxy HbA. In contrast to liganded hemoglobin [*e.g.* PDB entries 1cmy, 1hab, 1abw and 1bbb (Smith *et al.*, 1991; Silva *et al.*, 1992; Schumacher *et al.*, 1997; Kroeger & Kundrot, 1997)], human deoxy HbA crystallizes under a variety of conditions (different pH, ionic strength and preci-

pitants) and the same relative basic T-state quaternary structure is observed using either PEG or concentrated salt as the precipitant (Arnone & Perutz, 1974; Ward *et al.*, 1975; Fermi *et al.*, 1984; Kavanaugh *et al.*, 1992; Richard *et al.*, 1993; Paoli *et al.*, 1996; Seixas *et al.*, 1999; Safo *et al.*, 2001).

Smith & Simmons (1994) reported that under physiological conditions (pH 7.4 and low ionic strength in the presence of PEG 8000) human cyanomet HbA adopts an intermediate (Y-like) structure, but coordinates for this structure were never published or deposited in the PDB. By altering crystallization conditions (low salt concentration, pH 5.8, PEG as a precipitant), Silva *et al.* (1992) identified a third quaternary structure of liganded human COHbA denoted as the R2 state, which was similar to the Y state reported for the mutant human Hb Ypsilanti (βD99Y; Smith *et al.*, 1991), but with significant differences. The magnitude of the spatial differences between the R and R2 states are as large as those between the R and T states; the R state is almost 'equidistant' from the T and R2 states; and the T–R2 state movements differ in direction compared with the T–R transition, yet are almost twice as large as those between the T and R states (Silva *et al.*, 1992). These differences are the consequences of alterations in the organization of the individual subunits within the hemoglobin tetramer and in many side-chain conformations, particularly at the $\alpha1\beta2$ interface and the β–β end of the central cavity (Silva *et al.*, 1992). For example, in the R state the $-$COOH termini exhibit high mobility. In the R2 state, the β1 and β2H146 imidazole side chains reposition, stacking against one another with the formation of a salt bridge between the α-carboxylate group of β2H146 and the β1K82 side chain (Silva *et al.*, 1992; Schumacher *et al.*, 1997). The effect is a folding over at the β—β end of the central cavity. In addition, there is also a difference in the associated water structure. Detailed structural comparisons of the R, R2 and T states have been presented by various authors (*e.g.* Silva *et al.*, 1992; Schumacher *et al.*, 1997; Vásquez *et al.*, 1998). It has also been suggested that the R2 structure is actually the end point in the transition state (T→R→R2), since the R2 structure may provide a means around a steric barrier from T to R (for further details, see Silva *et al.*, 1992; Srinivasan & Rose, 1994; Mueser *et al.*, 2000; Tame, 1999; Xu *et al.*, 2003).

Several other R2 hemoglobin crystal structures have since been reported, but none were at neutral pH (*e.g.* Mueser *et al.*, 2000). Since the red-cell cytosol is a relatively low ionic strength environment ($\sim$0.15 M) at neutral pH, one criticism is that the R2 state observed for human hemoglobin crystal structures has only been generated at non-physiological pHs (Tame, 1999). However, this argument is weakened by the recent NMR observation that human COHbA (pH 7.0, 0.1 M sodium phosphate buffer, 90% H_2O/10% D_2O) exhibits an R2-like quaternary structure (Lukin *et al.*, 2003). To date, the significance of the R2 structure in the allosteric transition and the *in vivo* quaternary form of liganded human hemoglobin, as it exists in the red blood cell, remain unresolved.

We report here the 2.1 Å resolution crystal structures of human liganded hemoglobins COHbC (β6 Glu→Lys; PDB code 1m9p) and COHbS (β6 Glu→Val; PDB code 1nej),

under conditions of neutral pH (7.1) and low ionic strength (Na HEPES buffer, PEG 4000 as the precipitant). These structures exhibit quaternary structures that are very similar to the R2 structure of COHbA (PDB code 1bbb) obtained at pH 5.8 in the presence of PEG 6000. To the best of our knowledge, these are the first detailed high-resolution R2 quaternary structures reported for human hemoglobins crystallized under conditions approaching physiological (neutral pH and low ionic strength). Of significance is that liganded HbA does not form crystals under these or similar conditions. Thus, the β6 mutant hemoglobins may be useful in the further exploration of the R2 state. Solubility and modeling studies suggest that specific lattice contacts contribute to the high propensity of the β6 mutants to form higher ordered aggregates and to the inability of COHbA to form crystals at neutral pH under these conditions.

2. Materials and methods

2.1. Protein purification, ligation and crystallization

Human hemoglobins A (E6E), C (E6K) and S (E6V) were purified from the blood of AA, CC and SC individuals and stripped as reported previously (Hirsch *et al.*, 1999). Samples were dialyzed against 50 mM Na HEPES buffer pH 7.1, concentrated to 120–180 mg ml^{-1} using Amicon 10K centrifugal concentrators, frozen in liquid nitrogen and stored at 138 K. Protein purity was verified by isoelectric focusing and native 12% PAGE gels. The absence of methemoglobin was confirmed by absorption spectroscopy (500–700 nm). Prior to crystallization, each stock of mother-liquor solution was saturated with carbon monoxide. The hemoglobins (20–40 µl in each aliquot) were gently exposed to carbon monoxide gas without bubbling. The handling of the hemoglobins is similar to that described in Hirsch *et al.* (1999).

For the solubility studies, COHbC, COHbS and their mixtures were crystallized by sitting-drop vapor diffusion. The protein concentration varied between 10 and 50 mg ml^{-1} and the PEG 4000 concentration varied from 5 to 45%. The solutions were buffered with 100 mM Na HEPES pH 7.1. Equal amounts (typically 2 µl each) of protein solution and mother liquor were mixed and quickly sealed under CO. All experiments were carried out at 298 K. The appearance of crystals or precipitates was monitored microscopically every 24 h for up to two weeks. Phase diagrams were constructed as a function of precipitant concentration and protein solubility.

For X-ray data collection, COHbC crystals were obtained under the conditions described above by sitting-drop vapor diffusion at 298 K from a solution of 10–20 mg ml^{-1} protein, using 0.1 M Na HEPES buffer (prepared by titrating Na HEPES with HCl to pH 7.1) and 20–21% PEG 4000 as precipitant. COHbS was crystallized in the same manner by mixing equal volumes of protein solution (30 mg ml^{-1}) and 0.1 M Na HEPES buffer pH 7.1 with 25% PEG 4000. Mixtures of COHbC and COHbS in different ratios, ranging from 9:1 to 1:1, were crystallized as described above with PEG 4000 (20–25%) and protein concentrations at 5–50 mg ml^{-1}.

Table 1
Space groups and unit-cell parameters for carbonmonoxy hemoglobin crystals.

PDB code	Crystallization conditions	Space group	Unit-cell parameters				Resolution (Å)	Quaternary state
			a (Å)	b (Å)	c (Å)	$\alpha = \beta = \gamma$ (°)		
1bbb (HbA)	10 mg ml^{-1} protein, 0.1 M cacodylate buffer pH 5.8, 16% PEG 6000, 0.075 M Cl$^-$	$P2_12_12_1$	97.50	101.70	61.1	90	1.7	R2
1k1k (HbC)	20 mg ml^{-1} protein, 1.75 M potassium phosphate pH 7.35	$P4_12_12$	54.16	54.16	195.30	90	2.0	R
1m9p (HbC)	10 mg ml^{-1} protein, 0.15 M Na HEPES pH 7.1, 25% PEG 4000, traces of Cl$^-$	$P2_12_12_1$	56.00	58.70	175.20	90	2.1	R2
1nej (HbS)	30 mg ml^{-1} protein, 0.15 M Na HEPES pH 7.1, 25% PEG 4000	$P2_12_12_1$	58.00	58.53	171.84	90	2.1	R2
Mixed crystals, ratio 3:2 HbC:HbS	10 mg ml^{-1} protein, 0.15 M Na HEPES pH 7.1, 25% PEG 4000, traces of Cl$^-$	$P2_12_12_1$	56.29	58.73	174.56	90	2.6	R2
Mixed crystals, ratio 9:1 HbC:HbS	10 mg ml^{-1} protein, 0.15 M Na HEPES pH 7.1, 25% PEG 4000, traces of Cl$^-$	$P2_12_12_1$	56.13	58.75	174.22	90	2.6	R2

Crystals were individually transferred to a fresh drop of mother liquor of the same or slightly higher concentration of PEG 4000 (to prevent rapid dissolution), washed three times and then transferred to a drop with distilled water. Dissolved crystals were further analyzed for the HbC:HbS ratio using native PAGE.

Crystals of COHbC usually appeared after 24 h and continued to increase in size during 5–6 d. At the time of data collection, the crystals were 48 h (COHbC), 4 d (COHbC: COHbS mixture in a 7:3 ratio) or 6 d old (COHbS). The washed and dissolved crystals did not contain a detectable amount of methemoglobin. COHbA or oxyHbA did not generate crystals under these conditions.

2.2. Structure solution

Before data collection, protein crystals were soaked for a few minutes in CO-saturated mother liquor containing 15 or 20% glycerol as a cryoprotectant. X-ray data were collected to 2.1 Å at 100 K from flash-frozen crystals of COHbC and COHbS using an RU-200 rotating-anode X-ray generator ($\lambda = 1.5418$ Å) coupled to a Rigaku R-AXIS IV area detector. All crystals belong to the orthorhombic space group $P2_12_12_1$, with very similar unit-cell parameters (Table 1), corresponding to a single hemoglobin tetramer per asymmetric unit. Data were indexed with *DENZO* and reduced with *SCALEPACK* (Otwinowski & Minor, 1997), resulting in R_{merge} values of 8.1 and 6.8% for COHbC and COHbS, respectively.

The structure of the COHbA tetramer (PDB code 1bbb) served as a starting model for molecular replacement using *X-PLOR* (Brünger, 1996). For the COHbC crystal structure, the cross-rotation function followed by PC refinement within the resolution range 15.0–4.0 Å yielded a single peak corresponding to a single hemoglobin tetramer within the asymmetric unit. Combined translation search and rigid-body refinement resulted in a model with an initial R_{free} and R_{work} of 0.45 and 0.38, respectively. The structure was further refined to

Table 2
Data-collection and refinement statistics.

	COHbC	COHbS
Diffraction data		
Space group	$P2_12_12_1$	$P2_12_12_1$
Resolution range (Å)	2.1–20.0	2.1–20.0
Completeness (%)	90	91.7
$R_{merge}(I)$	0.081	0.068
No. of unique reflections		
All	32840	35224
Observed	31220	32283
Structure refinement		
Resolution range (Å)	2.1–8.0	2.1–8.0
R_{cryst} (%)	0.231	0.235
R_{free} (%)	0.269	0.268
No. of protein atoms	4384	4380
No. of heteroatoms	180	180
No. of solvent atoms	437	232
Average B factor (Å^2)		
Protein atoms	51.72	53.00
R.m.s. deviations from ideal value		
Bonds (Å)	0.013	0.013
Angles (°)	1.764	1.751

2.1 Å resolution by simulated-annealing, positional and individual isotropic B-factor refinement. Some errors in the model were corrected manually using *TOM*3.2 graphics software. When the R_{free} value fell below 0.29, water molecules were added to 3.0σ features in the $F_o - F_c$ electron-density map. After bulk-solvent correction (Brünger, 1996), the final R_{work} and R_{free} values were 0.231 and 0.269, respectively.

The coordinates for COHbC served as the starting model for refinement of the COHbS structure. Refinement was carried out essentially in the same way as for COHbC and yielded final R_{work} and R_{free} values of 0.235 and 0.268, respectively. All refinement statistics data are presented in Table 2.

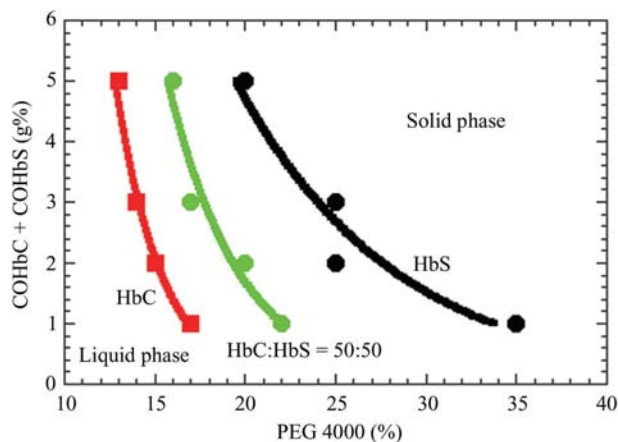For modeling studies, the *Insight*II software (Accelrys, San Diego, CA, USA) was used.

Figure 1
Solubility plots for COHbC (red), COHbS (black) and their mixture in a 1:1 ratio (green) in 0.1 M HEPES pH 7.1 with PEG 4000 as a precipitant.
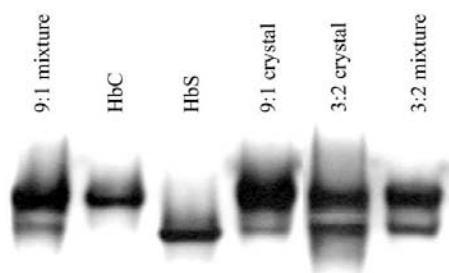

Figure 2
Separation of hemoglobins from dissolved crystals of HbC, HbS and their mixtures on native PAGE without detergents (see §2). For better viewing, the gel was stained using Bio-Rad Coomassie stain solution, although red bands for hemoglobins were observed prior to staining.
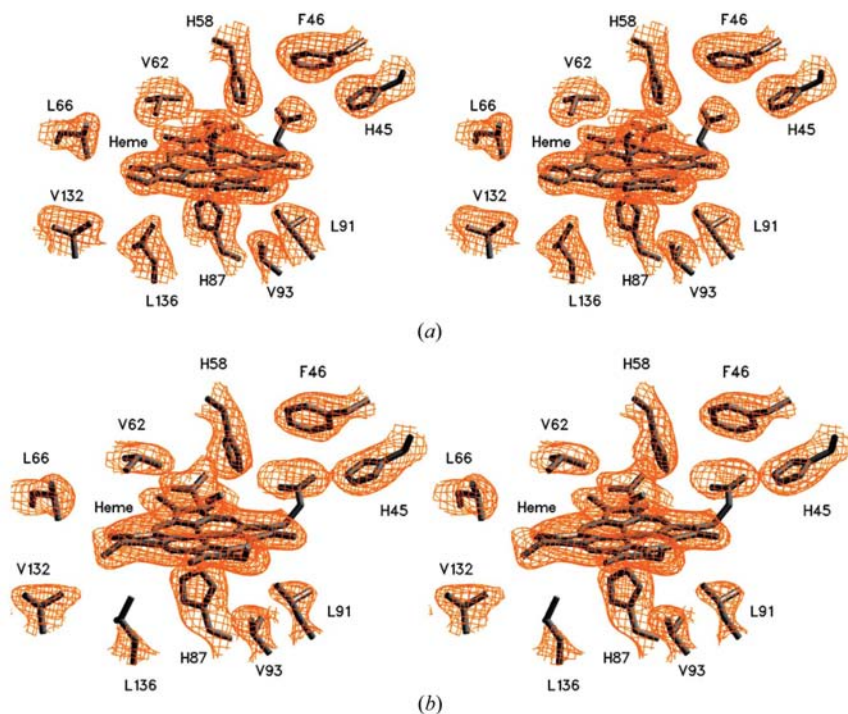

Figure 3
α-Heme electron density. The hemes were omitted in the calculations of the maps. Stereoview of $2F_o - F_c$ electron-density omit maps (2σ cutoff) drawn around α-hemes and surrounding amino-acid side chains for the R2-state structures of COHbC (a) and COHbS (b). (See Table 1 for space-group and unit-cell parameters and Table 2 for data-collection and refinement statistics.)

3. Results

3.1. Solubility studies

The pathologic ordered aggregation of the β6 mutant hemoglobins may be viewed as a consequence of altered protein solubility. To determine the mechanisms that give rise to liganded HbC crystallization, solubility studies for COHbC and COHbS and their mixtures were conducted under conditions of neutral pH and low ionic strength. COHbC exhibits a markedly lower solubility than COHbS at pH 7.1 under low ionic strength conditions (Fig. 1). Mixtures of both types of hemoglobin resulted in an intermediate solubility falling between the solubility plots of solutions of COHbC and COHbS alone (Fig. 1). Increasing the ratio between HbC:HbS from 1:1 to 9:1 shifts the solubility plots toward that of COHbC, indicating decreasing solubility (not shown). The ratio of COHbC:COHbS in solution was retained in the crystals, as demonstrated by native PAGE (Fig. 2). HbA did not form crystals under these solvent conditions and time duration. Crystals could be maintained under a renewed CO atmosphere for up to a month without significant heme oxidation.

The Gibbs free energy of crystallization is typically calculated using the formalism

$$\Delta G_{\text{cryst}} = -RT \ln C,$$

where C is the molar protein concentration where equilibrium is reached between the solid and liquid phase (Vekilov et al., 2002). To compare ΔG_{cryst} values for different proteins, protein concentrations applied to this equation have to be under identical crystallization conditions. Applying the method of Vekilov et al. (2002) to our solubility data,

$$\Delta\Delta G_{\text{cryst}} = RT \ln(C_{\text{eq}}\text{HbS}/C_{\text{eq}}\text{HbC}),$$

the differential free-energy change ($\Delta\Delta G$) for crystallization between COHbC and COHbS is approximated to be -5.0 kJ mol^{-1}. These values are less than would be expected for moderate ionic interaction (e.g. a salt bridge).

3.2. Crystallization and co-crystallization of COHbC and COHbS

COHbC and COHbS crystals formed within a wide pH range (5.6–8.5) with different PEGs as precipitants, including 0.1 M Na HEPES pH 7.1 and PEG combinations. In contrast to the β6 mutants, COHbA produced very few types of crystals in the presence of high-salt buffers (ammonium sulfate or sodium phosphate) and no crystals were observed at neutral pH and low ionic strength using PEGs as precipitants.

HEPES buffer is employed in both the above solubility studies and crystallography

Table 3
R.m.s. differences between the T, R and R2 states for human hemoglobins *versus* the R2 state of COHbC.

R.m.s.d. between C^{α} atoms only.

	Quaternary state	R.m.s.d.† (Å)						
		α_1 *versus* α_1	α_2 *versus* α_2	β_1 *versus* β_1	β_2 *versus* β_2	$\alpha_1\beta_1$ *versus* $\alpha_1\beta_1$	$\alpha_2\beta_2$ *versus* $\alpha_2\beta_2$	$\alpha_1\beta_1\alpha_2\beta_2$ *versus* $\alpha_1\beta_1\alpha_2\beta_2$
DeoxyHbA (PDB code 2hhb)	T	0.58	0.66	0.85	0.82	0.93	0.91	3.56
COHbC (PDB code 1k1k)	R	0.48	0.53	0.43	0.46	0.51	0.54	1.73
COHbS (PDB code 1nej)	R2	0.38	0.37	0.38	0.40	0.39	0.40	0.45
COHbA (PDB code 1bbb)	R2	0.36	0.39	0.44	0.49	0.42	0.46	0.48
O_2HbA (PDB code 1hho)	R	0.49	0.53	0.46	0.49	0.51	0.55	1.69

† For α-chains without the last three residues and for β-chains without the last five residues.

as earlier solution conformational studies of these mutants utilized this buffer system (*e.g.* Hirsch *et al.*, 1999). Moreover, hemoglobin in phosphate buffer is no longer considered to be a truly 'stripped' hemoglobin structure (*i.e.* devoid of inorganic phosphate and effectors that bind to hemoglobin). This has recently been corroborated by crystallography (Safo & Abraham, 2001).

X-ray diffraction studies were performed on crystals obtained from pure HbC or HbS and on crystals obtained from mixtures (Tables 1 and 2). As noted above, mixtures of COHbC and COHbS form single crystals (co-crystallize) and retain the Hb proportionality (Figs. 1 and 2).

3.3. Quaternary conformation of COHbC and COHbS

The quality of each structure (PDB codes 1m9p and PDB 1nej) is illustrated in Fig. 3, where the $2F_o - F_c$ electron-density maps for α hemes and surrounding residues are shown for COHbC (Fig. 3*a*) and COHbS (Fig. 3*b*). In order to assess the tertiary and quaternary structures present in these structures, the coordinates of the models were aligned with those previously determined for the R and R2 states of liganded HbA (Table 3 and Fig. 4). Of particular note, the present structures exhibit the R2 quaternary signature conformation of the $\alpha_1\beta_2$ interface (Fig. 5) and the central cavity as characterized by Silva *et al.* (1992).

The r.m.s. difference between C^{α} atoms for pairs of α and β chains and $\alpha_1\beta_1$ or $\alpha_2\beta_2$ heterodimers for different R-state structures are close to the experimental coordinate error determined for COHbC (PDB code 1m9p; 0.38 Å) and COHbS (PDB code 1nej; 0.3 Å). In contrast, a comparison of the current COHbC R2 structure with the T state (PDB code 2hhb) exhibits a significant 0.91 Å r.m.s. difference (Table 3).

Comparisons of the r.m.s. coordinate differences between hemoglobin tetramers indicate that COHbC and COHbS crystallized under low-salt conditions adopted the quaternary R2 state. The r.m.s.d. between C^{α} atoms comparing the COHbC R2 state (PDB code 1m9p) with the COHbA R2 state (PDB code 1bbb; Silva *et al.*, 1992) and with COHbS (PDB code 1nej) was 0.48 and 0.45 Å, respectively (Table 3). These results obtained at low ionic strength are in contrast to the high-resolution structure for COHbC crystallized in concentrated sodium phosphate, which is indistinguishable from the

R state of oxyHbA (PDB code 1k1k; Dewan *et al.*, 2000; Table 3).

4. Discussion

Superimposition of C^{α} atoms of Hb tetramers in the T, R and R2 states provides evidence that the crystal structures presented here for COHbC and COHbS (obtained at neutral pH and low ionic strength) are very similar to the R2 quaternary state (Table 3 and Fig. 4). This is further confirmed by the detailed likeness of the COHbC and COHbS quaternary conformations of the $\alpha_1\beta_2$ interface (Fig. 5) and the central cavity to those of the R2 state (Silva *et al.*, 1992).

The R2 central cavity domain exhibits one of the most significant structural differences between the R2 and R states. R2 structures obtained by others at non-neutral pH show a repositioning of the β_1 and β_2H146 imidazole side chains that stack against one another, along with the formation of a salt bridge between β_2H146 and β_1K82 (Silva *et al.*, 1992; Schumacher *et al.*, 1997). However, the C-termini of the β subunits of R2 COHbC and COHbS (PDB codes 1m9p and 1nej) show greater flexibility, which is reflected by poorly defined electron density and higher than average B factors. These observations suggest that at neutral pH values there are no strong interactions between the β-chain C-terminus within the β-cleft of the R2 structure. It is possible then that this greater flexibility may enable the β-chain C-terminus to play a special dynamic role as the gate to the central cavity, which would explain the established binding of allosteric effectors to liganded hemoglobin (*e.g.* Yonetani *et al.*, 2002).

As expected, based on the COHbC structure from concentrated phosphate (PDB code 1k1k) and the deoxy HbS structure (PDB code 2hbs), the respective A helix containing the βK6 (and βV6) side chains of these COHbC (and COHbS) R2 structures appear to be flexible, with high B factors and without clear density. However, modeling studies show βK6 to be localized closest to βE22 and in the proximity of βE26 and βH117 of a crystallographically related HbC or HbS tetramer (Fig. 6*a*). Regarding COHbS, modeling shows that βV6 has a shorter non-polar side chain (Fig. 6*b*) and therefore is not involved in direct molecular interactions in the crystal (*e.g.* more than 5 Å from polar residues in symmetry-related molecules). Therefore, since βV6 is distant from the

crystallographically related Hb tetramer, the βV6 side chain is not involved in potentially favorable interactions such as are predicted for the βK6 side chain of HbC. These considerations and the variety of possible rotameric conformations affording interactions with several residues may account for the small crystallization energy difference (Δ5 kJ) between COHbC and COHbS. These predictions are also consistent with the HbC and HbS co-crystallization data: increasing the HbC ratio in the mixture results in lower solubility and *vice versa*. At the same time, co-crystallization of COHbC and COHbS in different ratios (Figs. 1 and 2) leads to the formation of similar crystal packing, indicating the presence of mixed lattice contacts involving both βK6 and βV6 (Table 1). This obser-

vation may be explained by lattice contacts involving βV6 being thermodynamically less favorable than those for βK6 COHbC, accounting for the intermediate energy value between COHbC and COHbS crystallization. Additionally, although βV6 does not make a direct contact, it is presumably in contact with solvent, filling a gap between the crystallographically related molecules. At the very least, although βV6 does alter the solubility (Fig. 1), it does not interfere with co-crystallization by accommodating both isoforms in the same lattice.

Regarding HbC, βK6 could potentially interact with βE22, βE26 and βH117 in a crystallographically related tetramer in our high-resolution structure of COHbC (R state) obtained in
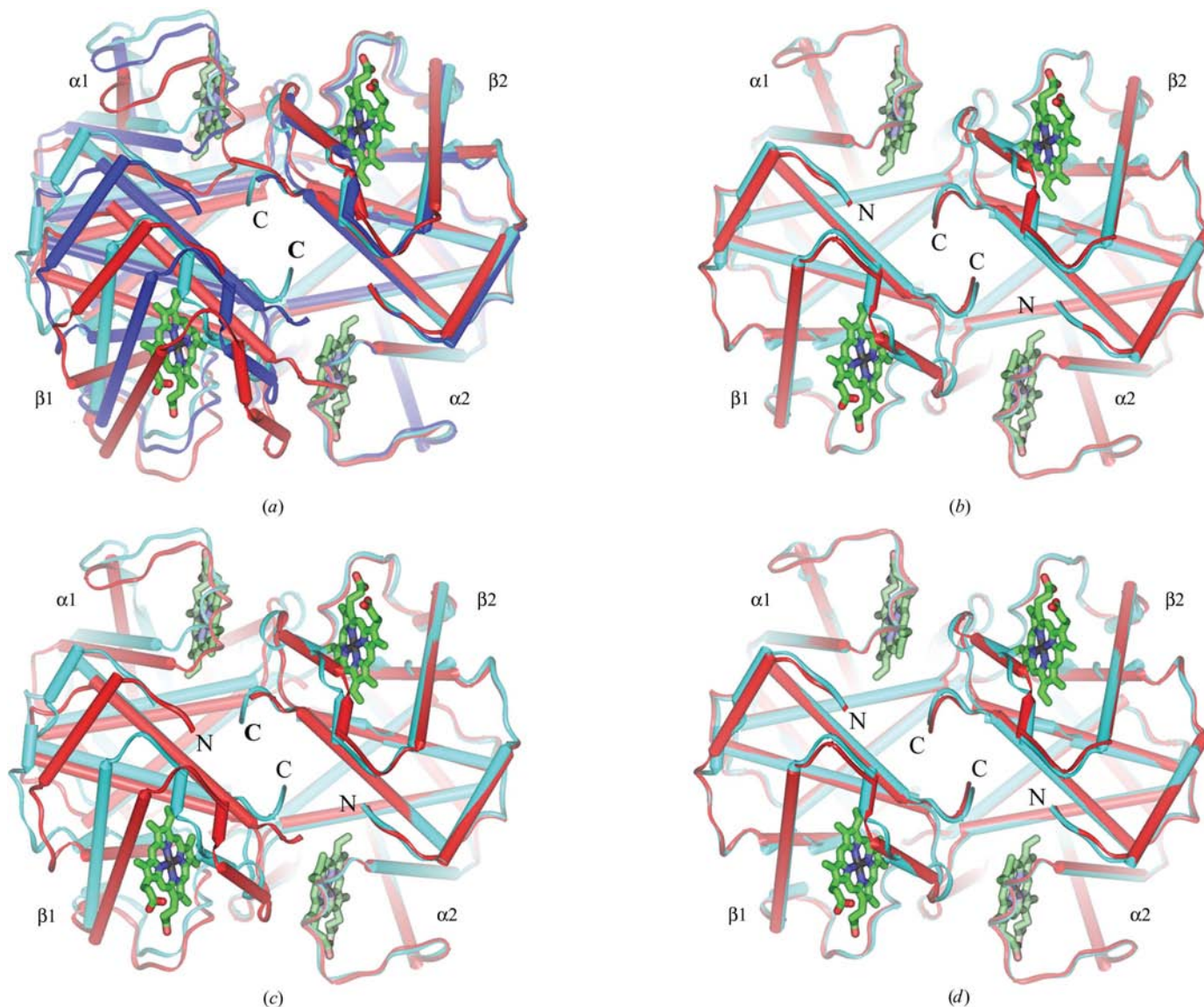

Figure 4
Superimposition of T, R and R2 structures of human hemoglobin. For this presentation, only coordinates for $\alpha1\beta1$ heterodimers were aligned for all PDB entries used, so that the position of the second heterodimer more clearly represents the quaternary transition within a tetramer as a shift of one heterodimer with respect to another. (*a*) Schematic representation of T–R–R2 transition. Coordinates for the T state (red) were from deoxyHbA (PDB code 2hhb), for the R state (dark blue) from oxyHbA (PDB code 1hho) and for the R2 state (light blue) from COHbA (PDB code 1bbb). (*b*) Superimposition of R2-state structures for COHbA (red; PDB code 1bbb) and COHbC (light blue; PDB code 1m9p). (*c*) Superimposition of two quaternary states for COHbC: the 'high-salt' R-state structure (red; PDB code 1k1k) and the 'low-salt' R2 state structure (light blue; PDB code 1m9p). (*d*) Superimposition of R2-state structures for COHbC (red; PDB code 1m9p) and COHbS (light blue; PDB code 1nej).

concentrated phosphate buffer (1.75 M potassium phosphate pH 7.35; PDB code 1k1k; Dewan *et al.*, 2000). In the R-state conformation of HbC, the βK6 side chain is located in closest proximity to βH117 (Dewan *et al.*, 2000), whereas in the R2 structure, βK6 is in closest proximity to βE22 (Fig. 6). Although data demonstrate that β6K is always involved in crystal lattice contacts, the two COHbC structures [R (Dewan *et al.*, 2000) and R2] exhibit different lattice contacts and different side-chain orientations. Nevertheless, the potential interaction of βK6 with these specific residues in either the R or R2 state may contribute to the mechanistic basis underlying the recent finding that liganded HbC exhibits a greater intermolecular attraction and longer range intermolecular attraction than liganded HbS and liganded HbA (Chen *et al.*, 2004).

Regarding HbA, since COHbA did not crystallize at neutral pH under these low ionic strength conditions, the overall data point to differences in lattice contacts and thermodynamics to explain the unique propensity of liganded HbC to form crystals. One explanation may be that β6E is in proximity to βE22 and βE26 (PDB code 1hho), possibly giving rise to unfavorable repelling interactions and thereby does not have the potential to form these weak symmetry contacts. This could explain the failure of crystallization attempts with COHbA under these or similar conditions. The one exception is the report by Smith *et al.* (1991): cyanomet HbA, crystallized at pH 7.4 (but in the presence of 0.1 M Tris–HCl, 0.1 M NaCl), formed the R2 quaternary structure with the same space group as reported here, but with different unit-cell parameters, implying different lattice contacts. It is unfortunate that the coordinates for the structure were never deposited and no other reports of or references to this structure have been found to date.

In brief, solubility and crystallographic studies of COHbC and COHbS provide an explanation for the high propensity of
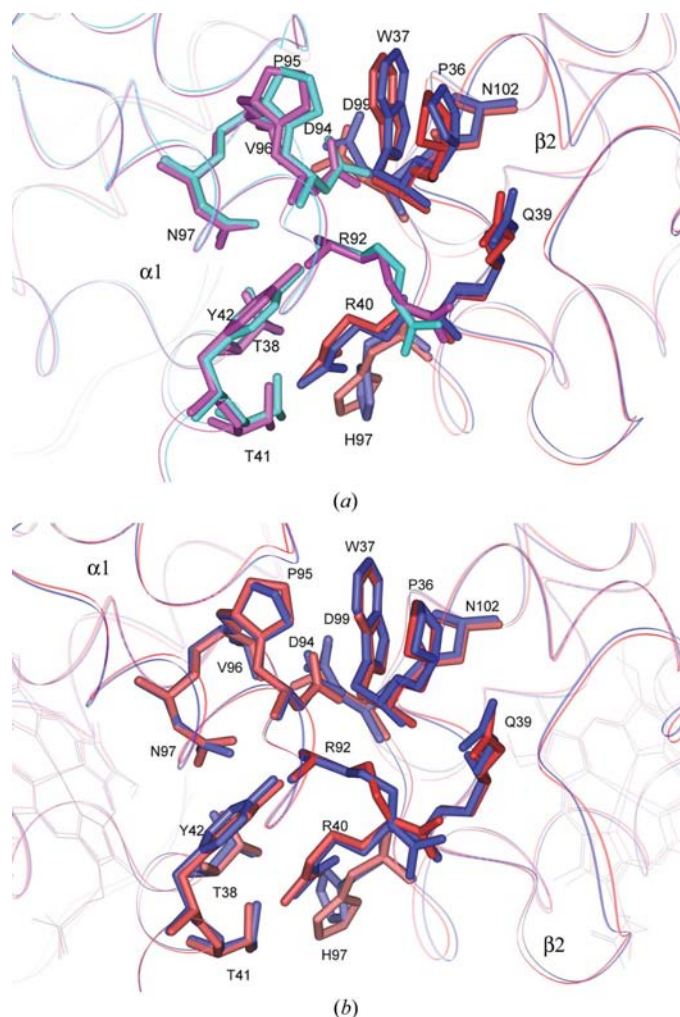

Figure 5
Dimer–dimer interactions within the $\alpha 1\beta 2$ interface of the R2 state. Overall structures are represented as ribbons and amino-acid side chains are drawn as sticks. (*a*) Superimposition of coordinates for R2 COHbC (light blue and dark blue; PDB code 1m9p) and R2 COHbA (pink and red; PDB code 1bbb). (*b*) Superimposition of coordinates for R2 COHbC (light blue and dark blue; PDB code 1m9p) and R2 COHbS (pink and red; PDB code 1nej).
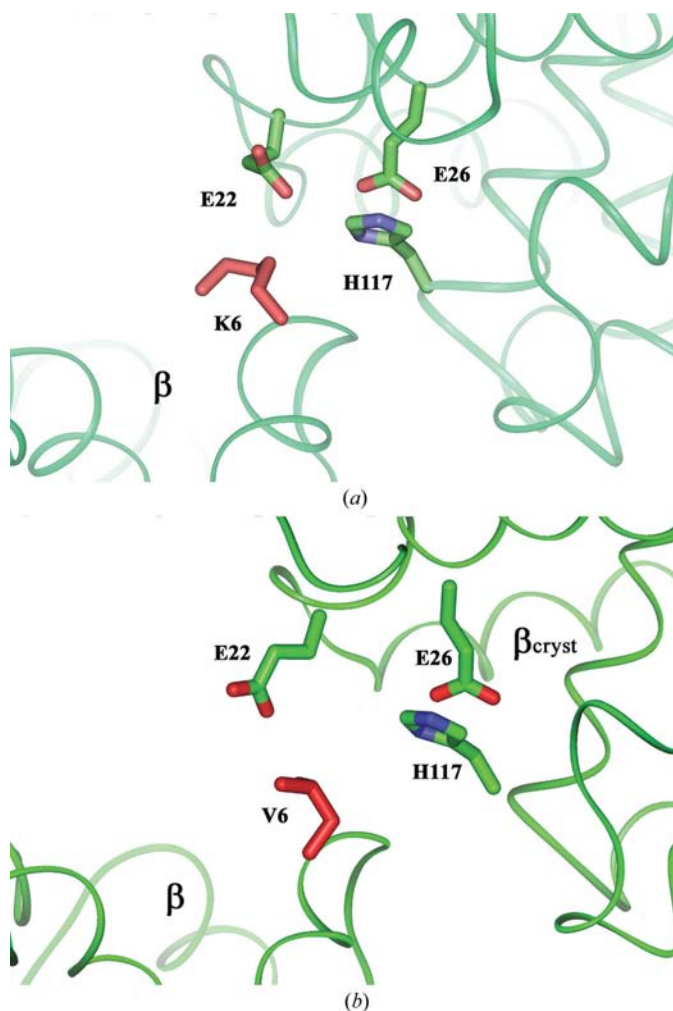

Figure 6
Crystallographic symmetry interactions involve residue β6 of HbC (*a*) and HbS (*b*) in the R2 state. Overall structures are represented as ribbons and side chains of residues along lattice contacts are drawn as stick models. The residue β6 is colored red and the remainder colored according to atom types: carbon, green; oxygen, red; nitrogen, blue. Residues are assigned using the single-letter code.

liganded HbC to crystallize. It is not yet clear what type of crystals may be formed by oxy HbC in human erythrocytes and the physiological relevance of the R2 state remains an open question. In this regard, since the low-concentration salt conditions at pH 7.1 (approaching physiological) yield the R2 quaternary state for human COHbC (and COHbS) and recent NMR solution studies of HbA identify the quaternary structure as R2-like (Lukin *et al.*, 2003), it would not be surprising if the intra-erythrocyte oxyHbC crystal exhibited the R2 quaternary form, further reflecting on the intra-erythrocytic Hb-liganded quaternary state.

References

Arnone, A. & Perutz, M. F. (1974). *Nature (London)*, **249**, 34–36.

Brünger, A. T. (1996). *X-PLOR Version 3.851. A System for X-ray Crystallography and NMR.* Yale University Press, New Haven, CT, USA.

Chen, Q. C., Vekilov, P. G., Nagel, R. L. & Hirsch, R. E. (2004). *Biophys. J.* **86**, 1702–1712.

Dewan, J. C., Feeling-Taylor, A., Puius, Y. A., Patskovska, L., Patskovsky, Y., Nagel, R. L., Almo, S. C. & Hirsch, R. E. (2002). *Acta Cryst.* D**58**, 2038–2042.

Fermi, G., Perutz, M. F., Shaanan, B. & Fourme, R. (1984). *J. Mol. Biol.* **175**, 159–174.

Hirsch, R. E., Juszczak, L. J., Fataliev, N. A., Friedman, J. M. & Nagel, R. L. (1999). *J. Biol. Chem.* **274**, 13777–13782.

Kavanaugh, J. S., Rogers, P. H., Case, D. A. & Arnone, A. (1992). *Biochemistry*, **31**, 4111–4121.

Koshland, D. E., Nemethy, G. & Filmer, D. (1966). *Biochemistry*, **5**, 365–385.

Kroeger, K. S. & Kundrot, C. E. (1997). *Structure*, **5**, 227–237.

Lukin, J. A., Kontaxis, G., Simplaceanu, V., Yuan, Y., Bax, A. & Ho, C. (2003). *Proc. Natl Acad. Sci. USA*, **100**, 517–520.

Monod, I., Wyman, I. & Changeaux, P. (1965). *J. Mol. Biol.* **12**, 88–118.

Mueser, T. C., Rogers, P. H. & Arnone, A. (2000). *Biochemistry*, **39**, 15353–15364.

Otwinowski, Z. & Minor, W. (1997). *Methods Enzymol.* **276**, 307–326.

Paoli, M., Liddington, R., Tame, J., Wilkinson, A. & Dodson, G. (1996). *J. Mol. Biol.* **256**, 775–792.

Perutz, M. F. (1970). *Nature (London)*, **228**, 726–739.

Puius, Y. A., Zou, M., Ho, N. T. & Almo, S. C. (1998). *Biochemistry*, **37**, 9258–9265.

Richard, V., Dodson, G. G. & Mauguen, Y. (1993). *J. Mol. Biol.* **233**, 270–274.

Safo, M. K. & Abraham, D. J. (2001). *Protein Sci.* **10**, 1091–1099.

Safo, M. K., Burnett, J. C., Musayev, F. N., Nokuri, S. & Abraham, D. J. (2002). *Acta Cryst.* D**58**, 2031–2037.

Safo, M. K., Moure, C. M., Burnett, J. C., Joshi, G. S. & Abraham, D. J. (2001). *Protein Sci.* **10**, 951–957.

Schumacher, M. A., Zheleznova, E. E., Poundstone, K. S., Kluger, R., Jones, R. T. & Brenan, R. G. (1997). *Proc. Natl Acad. Sci. USA*, **94**, 7841–7844.

Seixas, F. A. V., de Azevedo, W. F. Jr & Colombo, M. F. (1999). *Acta Cryst.* D**55**, 1914–1916.

Shaanan, B. (1983). *J. Mol. Biol.* **171**, 31–59.

Silva, M. M., Rogers, P. H. & Arnone, A. (1992). *J. Biol. Chem.* **267**, 17248–17256.

Smith, F. R, Lattman, E. E. & Carter, C. W. Jr (1991). *Proteins*, **10**, 81–91.

Smith, F. R. & Simmons, K. C. (1994). *Proteins*, **18**, 295–300.

Srinivasan, R. & Rose, G. D. (1994). *Proc. Natl Acad. Sci. USA*, **91**, 11113–11117.

Tame, J. R. H. (1999). *Trends Biol. Sci.* **24**, 372–377.

Vásquez, G. B., Ji, S., Fronticelli, C. & Gilliland, G. L. (1998). *Acta Cryst.* D**54**, 355–366.

Vekilov, P. G., Feeling-Taylor, A. R., Petsev, D. N., Galkin, O., Nagel, R. L. & Hirsch, R. E. (2002). *Biophys. J.* **83**, 1147–1156.

Ward, K. B., Wishner, B. C., Lattman, E. E. & Love, W. E. (1975). *J. Mol. Biol.* **98**, 161–177.

Xu, C., Tobi, D. & Behar, I. (2003). *J. Mol. Biol.* **333**, 153–168.

Yonetani, T., Park, S., Tsuneshige, A., Imai, K. & Kanaori, K. (2002). *J. Biol. Chem.* **277**, 34508–34520.